

Faktor mejne intenzitete napetosti pri počasnem natezanju navodičenega jekla z visoko trdnostjo

Threshold Stress Intensity Factor at Slow-Strain-Rate Tension of High-Strength Hydrogen-Charged Steel

B. Ule¹, F. Vodopivec¹, L. Vehovar¹ and L. Koscec²

Konstrukcijska jekla z visoko trdnostjo in visoko napetostjo tečenja se vedno bolj uporabljajo celo za izdelavo manj zahtevnih strojnih delov. Zaradi razmeroma nizke žilavosti tovrstnih jekel in slabo izraženega prehoda v krhko stanje postajajo toliko pomembnejše njihove lomne značilnosti.

Na izgubo lomne duktilnosti močno vpliva zlasti vodik v jeklu, čeprav pri tem ne učinkuje bistveno na napetost tečenja. Poslabšanje lomne duktilnosti pa je izrazito le pri počasnem natezanju navodičenega jekla, medtem ko ga pri konvencionalnem nateznem preizkusu skoraj ne zaznamo. Male koncentracije vodika v jeklu z visoko trdnostjo torej ne vplivajo na lomno žilavost takšnega jekla, peč pa imajo za posledico pojavljanje faktorja mejne intenzitete napetosti.

The use of structural steels with high-tensile and high-yield strength is increasing even in the manufacture of less demanding machine parts. Because of their relatively low toughness and poorly expressed transition into brittle state, their fracture properties are of major importance.

The decrease in fracture ductility is in particular strongly influenced by hydrogen content in steel, although hydrogen does not essentially affect its yield strength. However, the deterioration of fracture ductility is distinctive only at slow-strain-rate tension of hydrogen-charged steel, whereas it practically cannot be detected in a conventional tensile test. Consequently, the low concentration of hydrogen in high-strength steel does not influence its fracture toughness, but results in the appearance of a threshold stress intensity factor.

1. UVOD

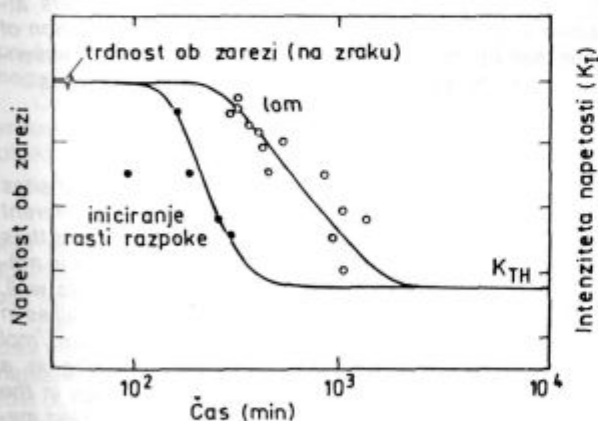
Ena od znanih oblik porušitve jekel z visoko trdnostjo je tako imenovani zapozneli lom statično obremenje-

1. INTRODUCTION

Delayed fracture caused by stress-induced hydrogen segregation is one of the known types of fracture of high-strength steel. This problem is characterised by the nucleation of a microcrack, which then grows until it achieves a critical size, resulting in an abrupt fracture (Fig. 1). The incubation period, as well as the delayed time to failure occurrence, are prolonged with the decrease in load until, at a sufficiently low load, the delayed failure does not occur. Therefore, we can speak of threshold of applied stress or threshold stress intensity factor K_{TH} , which can be considerably lower than the critical stress intensity factor or fracture toughness K_{IC} of steel. In the case of hydrogen embrittlement the threshold stress intensity factor is likewise denoted as K_{HE} .

The threshold stress intensity factor is inversely proportional to the hydrogen concentration in steel, which leads to the idea that the mutual effect of hydrogen and applied stress provokes the nucleation of microcracks. It was also found that the incubation period strongly depends on the hydrogen concentration in steel, while the effect of the applied stress magnitude is considerably lower.

Since the effect of hydrogen on the mechanical properties of high-strength steel is manifested by the decreased fracture ductility at slow-strain-rate tension and since such decrease depends on crack nucleation as well as on crack propagation, it is therefore logical that a slow-strain-rate tension test will by all means prove to



Slika 1:

Tipičen zapis pojava zapoznelega loma na nateznem preizkušancu z zarezo, obremenjenem s konstantno obremenitvijo. Zapis velja za vodičeno jeklo, vrisana pa je tudi trdnost ob zarezi za jeklo brez vodika (preizkušano na zraku) /lit. (1)/.

Fig. 1:

Typical delayed-failure phenomenon for hydrogen-charged notched tensile specimens at constant load.

The notch tensile strength of uncharged steel (measured in air) is also shown (Ref. 1).

¹ Inštitut za kovinske materiale in tehnologije, Lepi pot 11, 61000 Ljubljana

² Fakulteta za naravoslovje in tehnologijo, Oddelek za montanistiko, 61000 Ljubljana

^{*} Institute of metals and Technology, Lepi pot 11, 61000 Ljubljana

^{**} University of Ljubljana, Fac. of natural Science, Metal. dept., 61000 Ljubljana

nega jekla, ki je posledica napetostno inducirane segregiranja vodika v jeklu. Pri tem pojavu pride najprej do iniciiranja prve mikrorazpoke, ki nato počasi raste, vse dokler ne doseže kritične velikosti, kar povzroči hipno porušitev (sl. 1)¹. Inkubacijski čas kot tudi čas do loma se podaljšujeta z zniževanjem statično delujoče obremenitve, vse dokler pri neki dovolj nizki obremenitvi zapozneli lom izostane. Govorimo torej lahko o pragu delujoče napetosti oziroma o faktorju mejne intenzitete napetosti K_{TH} (threshold stress intensity factor), ki je lahko tudi občutno nižji od faktorja kritične intenzitete napetosti, to je od lomne žilavosti jekla K_{IC} . V razmerah vodikove krhkosti označimo faktor mejne intenzitete napetosti tudi kot K_{HE} .

Z znižanjem koncentracije vodika v jeklu se faktor mejne intenzitete napetosti zvišuje, kar napeljuje na misel, da je porajanje mikrorazpok posledica vzajemnega učinkovanja vodika in delujoče napetosti. Ugotovili so tudi², da je inkubacijski čas zelo odvisen od koncentracije vodika v jeklu, le malo pa od velikosti delujoče napetosti.

Ker se učinek vodika na mehanske lastnosti visokotrdega jekla manifestira z izgubo lomne duktilnosti pri počasnem natezanju in ker je lomna duktilnost jekla odvisna tako od porajanja kot tudi napredovanja razpok, je logično, da bo počasni natezni preizkus vsekakor primernejši za ugotavljanje vpliva vodika na lastnosti jekla kot pa konvencionalni natezni preizkus. Če je hitrost deformacije pri natezanju tako velika, da pride do loma v času, ki je krajši od inkubacijskega časa, učinek vodika na lastnosti jekla ne bo zaznaven.

Poleg statičnih preizkusov s konstantno obremenitvijo (static delayed failure test) se za določevanje občutljivosti jekla za lom, inducirani z vodikom, še največ uporablja natezni preizkus s cilindričnimi preizkušanci z zarezo po obodu. O tem priča opis Pollockove metode v reviji *Metals Progress*³. Pollock določa občutljivost jekla za lom, inducirani z vodikom, z merjenjem sile loma cilindričnih preizkušancev z zarezo po obodu pri hitrosti nateznaja $2 \times 10^{-4} \text{ mm s}^{-1}$. Trdnost zarezanega preizkušanca je namreč v takšnih primerih manjša od trdnosti gladkega, kar neposredno odseva izgubo duktilnosti zaradi učinkovanja vodika.

V strokovni literaturi je opisanih še več različnih načinov kvalitativnega določevanja občutljivosti jekla za lom, inducirani z vodikom, ki pa vsi temeljijo v glavnem na enostavnem merjenju stopnje poslabšanja kontrakcije pri natezanju jekla^{4, 5}.

Ker določevanje faktorja mejne intenzitete napetosti K_{TH} le na osnovi rezultatov nateznega preizkusa v literaturi še ni ustrezno obdelano, smo raziskali rešitev tega problema. Izkoristili smo merljivo poslabšanje lomne duktilnosti jekla pri počasnem natezanju kot nadomestku za dolgotrajni statični natezni preizkus pri konstantni obremenitvi. Ob tem smo upoštevali hipotezo, po kateri poslabšanje lomne duktilnosti pri počasnem natezanju dejansko potrjuje obstoj faktorja mejne intenzitete napetosti, če se lomna žilavost takšnega jekla - merjena pri običajnih hitrostih nateznaja - le malo ali pa sploh ne spremeni.

Razvoj in teoretična utemeljitev te metode omogočata določanje faktorja mejne intenzitete napetosti kar na osnovi rezultatov nateznega preizkusa, s tem pa je določevanje občutljivosti jekla za lom, inducirani z vodikom, bistveno bolj objektivno, kot je pri sedaj uporabljenih metodah.

2. TEORETIČNI DEL

Vodik je v železu v atomarni obliki bodisi na intersticijskih mrežnih mestih bodisi vezan v večji ali manjši me-

be more convenient in determining the influence of hydrogen on steel properties than a conventional tension test. If the deformation rate at tension is so large that failure occurs in a period shorter than the incubation one, the influence of hydrogen on the properties of steel will not be cognizable.

Besides static test at constant load (static delayed failure test), the tension test on cylindrical specimens with a circumferential notch is more frequently used for the determination of hydrogen induced fracture of steel. This is evident in the description of Pollock's method in *Metals Progress*³. Pollock determines the sensitivity of steel to hydrogen-induced fracture by measuring the fracture load at a crosshead speed of $2 \times 10^{-4} \text{ mm s}^{-1}$ using cylindrical notched tensile specimens. In this case the strength of notched specimens is lower than that of smooth specimens, which directly reflects the decrease of ductility due to the effect of hydrogen.

Many more methods for qualitative determination of hydrogen induced fracture of steel have been described in professional literature. However, all of these are mainly based on the measurement of the decrease of reduction of area at tension test of steel^{4, 5}. Since the determination of threshold stress intensity factor K_{TH} only on the basis of the results of a tensile test has not been adequately treated in literature, our attempts were aimed at finding a solution to this problem.

Instead of a long-term static test at constant load, we used the slow-strain-rate tension test for determining the measurable decrease in fracture ductility of steel. We followed the hypothesis that the decrease in fracture ductility at slow-strain-rate tension test actually confirms the existence of a threshold stress intensity factor if the fracture toughness of such steel - measured at conventional strain rate - changes only slightly or doesn't change at all.

The development and theoretical justification of this method prove its usefulness in determining the threshold stress intensity factor on the basis of results attained in a tensile test. In this way, the determination of steel sensitivity to hydrogen-induced fracture is essentially more objective than in currently used methods.

2. THEORY

Hydrogen is present in iron either at interstitial sites at the lattice or bound as trapped hydrogen to different discontinuities of the crystal lattice - "traps" - and thus referred to as trapped hydrogen. Some hydrogen in molecular form is always found in the microvoids as well. The partial molar volume of hydrogen in iron as well as in most other metals is surprisingly high (appr. $2 \text{ cm}^3/\text{mol}$ of hydrogen or $0,33 \text{ nm}^3/\text{atom}$)⁶⁻⁸. This results in a strong interaction between hydrogen interstitials in the crystal lattice and elastic-stress fields of the loaded metal lattice.

A thermodynamic analysis of this process, based on the assumption that hydrogen is a completely mobile component, was performed by Li, Oriani and Darken⁹, who found the following relation:

$$\mu - \mu_0 = \sigma_{ij} E_{ij} dV \quad (1)$$

The distortion field around the hydrogen atom is described by the deformation tensor E_{ij} ; ρ_{ij} is the stress tensor which determines the stress state originating from external loads acting on crystal lattice; μ_0 is the chemical potential of hydrogen in the absence of external stress, while u represents the chemical potential of hydrogen under external stress. The difference between

ri na različne diskontinuitete kristalne mreže, ki jih imenujemo s skupnim imenom pasti in od tod v pasteh ujeti vodik (trapped hydrogen). Nekaj vodika je v železu vedno tudi v porah v molekularni obliki. Parcialni molski volumen vodika v železu in večini drugih kovin je presenetljivo velik (približno 2 cm³/mol vodika, oziroma 0,33 nm³/atom)⁶⁻⁸. Posledica tega je močna interakcija med vodikovimi intersticijami v kristalni mreži ter polji elastičnih napetosti v obremenjeni kristalni mreži kovin.

Li, Oriani in Darken⁹, so s termodinamično analizo tega problema, pri čemer so vodik v železu obravnavali kot povsem mobilno komponento, prišli do izraza:

$$\mu - \mu_0 = \sigma_{ij} E_{ij} dV \quad (1)$$

Deformacijski tenzor E_{ij} opisuje deformacijsko polje okrog intersticijskega atoma vodika, μ_{ij} je napetostni tenzor, ki opredeljuje napetostno stanje, izvirajoče od zunanje mehanske obremenitve kristalne mreže. Z μ₀ je v zgornjem izrazu (1) označen kemijski potencial vodika v neobremenjeni kristalni mreži kovine, μ pa je kemijski potencial vodika v mehansko obremenjeni mreži kovine. Razlika potencialov je zato enaka delu, ki je potrebno za vgnezdenje intersticijskega vodika v polje delujočih napetosti.

Gradient napetosti torej povzroči gradient kemijskega potenciala vodika, le-ta pa predstavlja gonilno silo za difuzijo intersticijsko raztopljenega vodika. Rezultat tega je segregiranje vodika v neenakomernem polju napetosti: vodik se zaradi reverzibilne dilatacije kristalne mreže s pripadajočo pozitivno spremembo volumna, ki spremlja vgnezdenje vodikovih intersticij, koncentrira v področjih prevladujočih nateznih napetosti, medtem ko se področja s prevladujočimi tlačnimi napetostmi z vodikom osiromašijo. Prerazporejanje vodika v obremenjeni kristalni mreži poteka toliko časa, dokler ni dosežena v vseh točkah mreže ravtežna koncentracija vodika, določena z izrazom:

$$[H] = [H]_0 \exp \frac{\sigma_{ij} E_{ij} dV}{RT} \quad (2)$$

pri čemer je [H]₀ koncentracija enakomerno porazdeljenega vodika v neobremenjeni kristalni mreži.

Če upoštevamo le volumsko spremembo v okolici vrinjenih vodikovih atomov, lahko izraz (2) zapišemo v obliki:

$$[H] = [H]_0 \exp \frac{\sigma_m \bar{V}_H}{RT} \quad (3)$$

kjer je z σ_m označena hidrostatična komponenta napetostnega tenzorja (σ_m = 1/3 (σ_x + σ_y + σ_z)), V_H pa je parcialni molski volumen vodika v železu.

Z enačbo (3) je mogoče izračunati koncentracijo vodika v lokaliziranem področju, na primer v zoženem vratu nateznega preiskovanja, kjer deluje hidrostatična napetost σ_m. Ko koncentracija vodika [H] na tem mestu doseže kritično vrednost [H]_{cr}, ko je torej K₁ = K_{TH}, moramo računati z iniciiranjem mikrorazpok in zapoznelim lomom jekla. Problem je analitično rešil Gerberich¹⁰, ki je za faktor mejne intenzitete napetosti izpeljal izraz:

$$K_{TH} = \frac{RT}{\alpha \bar{V}_H} \ln \frac{[H]_{cr}}{[H]_0} - \frac{\sigma_{ys}}{2\alpha} \quad (4)$$

pri tem ima α eksperimentalno ugotovljeno vrednost 2/5 mm^{-1/2}.

Ovisnost (4) je eksperimentalno dobro potrjena, vendar pa pri napetostih tečenja, ki so nižje od 1200 MPa, pogosto prihaja do neujemanja med enačbo (4) in rezultati eksperimentov. To neujemanje lahko deloma razložimo z odvisnostjo razmerja [H]_{cr}/[H]₀ od napetosti tečenja jekla. Farrell and Quarrell⁴ sta namreč ugo-

the potentials is the work needed to place the hydrogen into the active stress field.

The gradient of chemical potential of hydrogen is therefore caused by the stress gradient and represents the driving force for the diffusion of interstitially dissolved hydrogen, resulting in hydrogen segregation in non-uniform stress field. Hydrogen concentrates in the areas of predominantly tensile stresses due to the reversible dilations of the crystal lattice with the corresponding volume changes accompanied by the insertion of hydrogen interstitials, while the compressively strained regions become impoverished with hydrogen. The redistribution of hydrogen in the strained crystal lattice takes place until an equilibrium concentration of hydrogen is achieved in all points of the crystal lattice. This is expressed by:

$$[H] = [H]_0 \exp \frac{\sigma_{ij} E_{ij} dV}{RT} \quad (2)$$

where [H]₀ is the concentration of hydrogen, uniformly distributed within the unstrained crystal lattice.

If only the volume change around the inserted hydrogen atoms is considered, the equation (2) may be expressed as:

$$[H] = [H]_0 \exp \frac{\sigma_m \bar{V}_H}{RT} \quad (3)$$

where σ_m is the hydrostatic component of stress tensor σ_m = 1/3 (σ_x + σ_y + σ_z) and V_H is the partial molal volume of hydrogen in iron.

Equation (3) may be used to calculate the concentration of hydrogen in a localised area, as for example in the narrowed neck of tensile specimens with hydrostatic stress σ_m.

Microcracks nucleation and delayed fracture of steel can be expected when the hydrogen concentration [H] in this region achieves the critical value [H]_{cr}, i.e. when K₁ = K_{TH}. This problem was solved analytically by Gerberich¹⁰, who expressed the threshold stress intensity factor in the form of:

$$K_{TH} = \frac{RT}{\alpha \bar{V}_H} \ln \frac{[H]_{cr}}{[H]_0} - \frac{\sigma_{ys}}{2\alpha} \quad (4)$$

where factor α reaches the experimentally determined value of 2/5 mm^{-1/2}.

The relation (4) is experimentally well confirmed, although some discrepancies can often be observed between Eq. (4) and the experimental results at yield strength below 1200 MPa. These discrepancies can be partly explained by the dependance of the [H]_{cr}/[H]₀ ratio on the yield point. Namely Farrell and Quarrell⁴ ascertained that larger concentrations of hydrogen are needed to produce embrittlement in steel with lower yield strength, which they expressed with the relation [H]_{cr} ∝ 1/σ_{ys}.

Kim and Loginow¹¹ proved that the content of soluble hydrogen in steel was proportional to the yield strength, thus [H]₀ ∝ σ_{ys}. If both statements are taken into account this can be written as:

$$\frac{[H]_{cr}}{[H]_0} \approx \frac{\beta}{\rho_{ys}} \quad (5)$$

where β is a constant for specific types of steel with determined hydrogen concentration.

By substituting (5) for (4), we arrive at the well-known Gerberich equation for threshold stress intensity factor in its final form:

$$K_{TH} = \frac{RT}{\alpha \bar{V}_H} \ln \frac{\beta}{\sigma_{ys}} - \frac{\sigma_{ys}}{2\alpha} \quad (6)$$

točila, da so ze doseganje krhkosti v jeklih z nižjo nape-
testjo tečenja potrebne višje koncentracije vodika, kar
sta zapisala kot $[H]_{cr} \propto 1/\sigma_{ys}$. Kim and Loginow¹¹ pa sta
dokazala, da se v jeklih z višjo napetostjo tečenja topi
več vodika, torej $[H]_0 \propto \sigma_{ys}$. Z upoštevanjem obeh naved-
denih ugotovitev lahko zapišemo:

$$\frac{[H]_{cr}}{[H]_0} \approx \frac{\beta}{\rho_{ys}} \quad (5)$$

pri čemer je β konstanta za posamično vrsto jekla in za
določeno vsebnost vodika v njem.

Ko substituira (5) v (4), dobimo znano Gerberic-
hovo enačbo za faktor mejne intenzitete napetosti v nje-
ni končni obliki:

$$K_{TH} = \frac{RT}{\alpha \bar{V}_H} \ln \frac{\beta}{\sigma_{ys}} - \frac{\sigma_{ys}}{2\alpha} \quad (6)$$

Ker vodik v jeklu še najbolj vpliva na lomno duktilnost
jekla pri počasnem natezanju, je za nadaljnjo teoretično
analizo smiselno poiskati soodvisnost med lomno žila-
vostjo K_{IC} in parametri nateznega preizkusa. Takšno so-
odvisnost poznamo pod imenom Hahn-Rosenfieldova
korelacija^{12,13}, ki ima naslednjo obliko:

$$K_{IC} = \sqrt{\frac{0,05 E_f n^2 E \sigma_{ys}}{3}} \quad (\text{MPa m}^{1/2}) \quad (7)$$

Pri tem je E_f lomna duktilnost, ki jo izračunamo iz
znane kontrakcije jekla Z po formuli:

$$E_f = \ln [1/(1-Z)] \quad (8)$$

medtem, ko eksponent deformacijskega utrjevanja n iz-
računamo iz enakomernega raztezka e_u po formuli:

$$n = \ln (1 + e_u) \quad (9)$$

Ker pri običajnih hitrostih obremenjevanja, kakršne
uporabljamo pri merjenju faktorja kritične intenzitete na-
petosti K_{IC} , ne zaznamo opaznejšega poslabšanja duktil-
nosti jekla, ki bi ga sicer lahko pripisali vplivu majhnih
koncentracij vodika v jeklu (okoli 1 ppm)^{4,14}, se zdi ute-
meljena hipoteza, da poslabšanje lomne duktilnosti jekla
pri počasnem natezanju dejansko odraža eksistenco
faktorja mejne intenzitete napetosti K_{TH} .

V skladu s to hipotezo bi lahko Hahn-Rosenfieldovo
korelacijo (7) uporabili kar za izračunavanje faktorja K_{TH} ,
potem ko bi v enačbo (7) vstavili vrednosti, izmerjene pri
počasnem natezanju. Ker pa je poznana tudi teoretično
izpeljana Gerberichova enačba za K_{TH} (6), v kateri je ne-
znana le vrednost β , je mogoče po izenačenju enačb (6)
in (7) vrednost β izraziti eksplicitno:

$$\beta = \sigma_{ys} \exp \frac{\alpha \bar{V}_H}{RT} \left\{ \sqrt{\frac{0,05 E_f n^2 E \sigma_{ys}}{3}} + \frac{\sigma_{ys}}{2\alpha} \right\} \quad (10)$$

V izrazu (10) so veljavne vrednosti za σ_{ys} , E_f ter n , kot
že rečeno, izmerjene pri počasnem nateznem preizkusu.

Verificiranje postavljene hipoteze se bo torej reducira-
lo na ugotavljanje konstantnosti veličine β , ki mora biti
neodvisna od napetosti tečenja jekla σ_{ys} . Konstantna
vrednost β pomeni, da je postavljena hipoteza pravilna in
da s podatki počasnega nateznega preizkusa lahko izra-
čunamo K_{TH} kar z enačbo (7).

3. EKSPERIMENTALNI DEL

Za eksperimentalno delo smo izbrali jeklo Č.4751 z
naslednjo kemijsko sestavo: 0,38% C, 0,99% Si, 0,38%
Mn, 0,012% P, 0,010% S, 5,19% Cr, 1,17% Mo ter 0,23%
V. Po homogenizacijskem žarjenju in normalizaciji smo
iz kovanih palic s premerom 16 mm za natezni preizkus

Since hydrogen in steel mostly affects the fracture
ductility at slow-strain-rate tension, it would therefore
seem adequate for further analysis to determine the re-
lation between fracture toughness K_{IC} and the param-
eters of tensile test. Such a relation, known as the Hahn-
Rosenfield correlation^{12,13}, is given by:

$$K_{IC} = \sqrt{\frac{0,05 E_f n^2 E \sigma_{ys}}{3}} \quad (\text{MPa m}^{1/2}) \quad (7)$$

where E_f is the fracture ductility, calculated from the ac-
tual reduction of area Z using the equation:

$$E_f = \ln [1/(1-Z)] \quad (8)$$

whereas the strain hardening exponent n can be calcu-
lated from the uniform elongation e_u using the equation:

$$n = \ln (1 + e_u) \quad (9)$$

Since the evident worsening of fracture ductility,
which may be attributed to the small amounts of hydrog-
en in steel (appr. 1 ppm), cannot be detected^{4,14} by con-
ventional strain-rate used in measurements of critical
stress intensity factor K_{IC} , it therefore seems that the hy-
pothesis according to which the decreased fracture
ductility at slow-strain-rate tension reflects the exist-
ence of threshold stress intensity factor is justified.

In accordance with this hypothesis, the Hahn-Rosen-
field correlation (7) could be used for the calculation of
 K_{TH} after the values measured at slow-strain-rate have
been inserted into equation (7). Since Gerberich's theo-
retically developed equation for K_{TH} (6) is also known (β
being the only unknown value), it is therefore possible to
express the value of β explicitly after the balance of Eq.
(6) and (7):

$$\beta = \sigma_{ys} \exp \frac{\alpha \bar{V}_H}{RT} \left\{ \sqrt{\frac{0,05 E_f n^2 E \sigma_{ys}}{3}} + \frac{\sigma_{ys}}{2\alpha} \right\} \quad (10)$$

As already mentioned, the relevant values of σ_{ys} , E_f
and n in Eq. (10) are measured in a slow-strain-rate ten-
sion test.

The verification of the postulated hypothesis will thus
be reduced to the measurement of constancy of the β
value, which has to be independent of the yield stress
 σ_{ys} of steel. The constant β value means that the hy-
pothesis is correct and that K_{TH} can be calculated using the
Eq. (7) on the basis of slow-strain-rate tensile test data.

3. EXPERIMENTAL

Steel Č.4751 containing (wt-%) 0,38% C, 0,99% Si,
0,38% Mn, 0,012% P, 0,010% S, 5,19% Cr, 1,17% Mo and
0,23% V has been chosen for experimental work. Cylin-
drical tensile specimens with a diameter of 10 mm,
gauge length of 100 mm and total length of 250 mm
were machined from the forged rod after it had been
homogeneously annealed and normalized. Specimens
were thermally treated in a vacuum annealing furnace.
They were austenitised at 980°C for a short period,
quenched in a flow of gaseous nitrogen and then tem-
pered at temperatures of 620°C, 640°C and 670°C re-
spectively. Thus, three separate and distinct classes of
yield strength - 1220 MPa, 1020 MPa and 900 MPa re-
spectively were achieved.

The cathodic charging of thermally treated tensile
specimens was carried out for 1 hour in 1 N sulfuric acid
at a current density of 0,3 mA/cm². The experimental
set-up for cathodic polarisation of tensile specimens, as
shown in Fig. 2, is composed of a potentiostat and cor-
rosion cell with electrodes.

izdelali 250 mm dolge cilindrične preiskušance s premerom 10 mm in dolžino 100 mm. Preiskušance smo toplotno obdelali v vakuumski žarilni peči, tako da smo jih po kratkotrajni austenitizaciji pri 980°C kalili v toku plinastega dušika, nato pa popuščali pri temperaturah 620°C, 640°C oziroma 670°C. Na ta način smo dobili tri ločene in dobro definirane trdnostne razrede z napetostjo tečenja 1220 MPa, 1020 MPa oziroma 900 MPa.

Toplotno obdelane preiskušance za natezni preizkus smo navodili z enournim katodnim polariziranjem v 1 N raztopini žveplene kisline pri gostoti toka 0,3 mA/cm². Eksperimentalni sklop s katodnim polariziranjem preizkušancev, sestavljen iz potenciostata in korozijske celice z elektrodami, je prikazan na sliki 2.

Natezne preizkuse smo opravili na nateznem trgalnem stroju INSTRON, potem ko smo natezne preiskušance po končanem navodičenju 24 ur zadrževali na zraku, da so se koncentracije vodika v jeklu približale residualnim vrednostim (približno 0,7 ppm), ki se nato časovno skoraj niso več spreminjale.

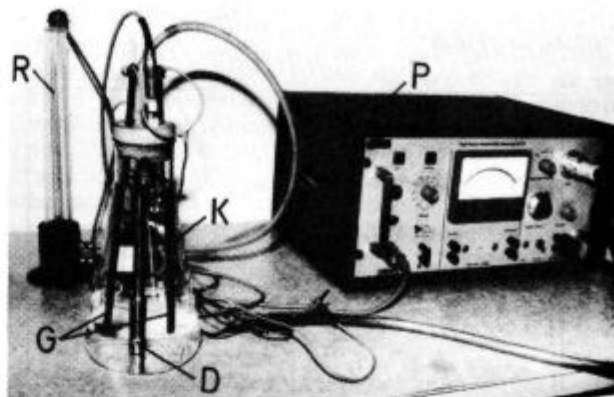
Za hitrost natezanja smo izbrali tako hitrost 1 mm/min, značilno za običajni natezni preizkus, kot tudi hitrost 0,1 mm/min, značilno za počasno natezanje. Merili smo napetost tečenja σ_{ys} (MPa), natezno trdnost σ_{TS} (MPa), maksimalni enakomerni raztezek e_u ($\times 100\%$) ter kontrakcijo jekla Z ($\times 100\%$).

Lomno duktilnost E_f in eksponent deformacijskega utrjevanja n smo izračunali z enačbama (8) in (9).

Mikrofraktografske preiskave prelomnih površin vodičenih in pri hitrosti natezanja 0,1 mm/min obremenjenih natezних preizkušancev smo opravili s scanning elektronskim mikroskopom JEOL JSM-35 (SEM).

4. REZULTATI

Izmerjene mehanske lastnosti navodičenega jekla kot tudi jekla brez vodika (pod 0,05 ppm) so zbrane v tabeli 1. V tej tabeli so zbrane še lomne žilavosti K_{IC} jekla, izračunane s Hahn-Rosenfieldovo korelacijo (7) na osnovi rezultatov običajnih natezних preizkusov pri hitrosti natezanja 1 mm/min ter nadalje še faktorji mejne intenzitete napetosti K_{TH} vodičenega jekla, izračunani z isto enačbo (7), vendar na osnovi rezultatov počasnega natezanja pri hitrosti 0,1 mm/min.



Slika 2: Eksperimentalni sklop za vodičenje natezних preiskušancev s katodnim polariziranjem. (P-potenciostat, D-natezni preizkušaneec, G-grafitni protielektrodi, K-kalomelova elektroda in R-rotameter).

Fig. 2: Experimental set-up for hydrogen charging of tensile specimens with cathodic polarisation. (P-potentiostat, D-tensile specimen, G-graphite electrodes, K-calomel electrode, R-rotameter).

The tension tests were made on an INSTRON testing machine, after hydrogen charging of specimens was completed and the specimens exposed to air for 24 hours. This enabled the concentrations of hydrogen in steel to approach the residual values (appr. 0.7 ppm), which remained nearly time-independent.

The tension tests were performed at conventional strain rate i.e. at a crosshead speed of 1 mm/min as well as at lower-strain-rate i.e. at a crosshead speed of 0.1 mm/min. The yield strength σ_{ys} (MPa), tensile strength σ_{TS} (MPa), max. uniform elongation e_u ($\times 100\%$) and the reduction of area Z ($\times 100\%$) were measured. The fracture ductility E_f and the strain hardening exponent n were calculated using equations (8) and (9) respectively.

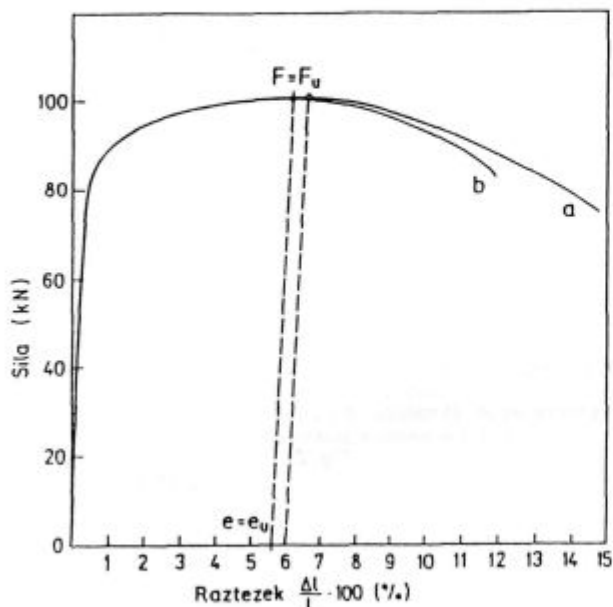
The fracture surfaces of tensile specimens tested at a crosshead speed of 0.1 mm/min were examined in the scanning electron microscope JEOL JSM-35 (SEM).

Tabela 1: Mehanske lastnosti jekla brez vodika in istega jekla po navodičenju

Table 1: Mechanical properties of uncharged and hydrogen-charged steel

Hitrost natezanja 1 min/min Crosshead speed 1 mm/min			Lomna žilavost Fracture toughness	Hitrost natezanja 0,1 mm/min Crosshead speed 0,1 mm/min			Faktor mejne inten. napet. Threshold stress inten. factor	Konstanta Constant
Napetost tečenja Yield strength σ_{ys} (MPa)	Enakomerni raztezek Uniform elongation $e_u \times 100\%$	Kontrakcija Reduction of area $Z \times 100\%$	K_{IC}	Napetost tečenja Yield strength σ_{ys} (MPa)	Enakomerni raztezek Uniform elongation $e_u \times 100\%$	Kontrakcija Reduction of area $Z \times 100\%$	K_{TH}	β /En (10)/ /Eq. (10)/ MPa
Jeklo brez vodika, uncharged steel								
924	8,7	52	126,9	910	8,5	51		
1010	7,4	51,3	112,5	1027	6,5	50,3		
1270	6,4	50	107,5	1214	6,2	50,3		
Navodičeno jeklo, hydrogen charged steel								
885	8,4	50,3	117,2	899	8,1	47,7	109,8	4005
1082	7,2	49,3	110,1	1078	6,5	42,7	90,1	4223
1209	6,1	47,3	96,3	1226	6,0	27,3	67,4	4037

V tabeli 1 so prikazane tudi vrednosti za konstanto β , izračunane s pomočjo enačbe (10) na osnovi rezultatov počasnega natezanja.



Slika 3:

Diagram sila-deformacija pri počasnem natezanju jekla trdnostnega razreda 1300 MPa; a) brez vodika (pod 0,05 ppm) in b) 24 ur po vodičenju (ca. 0,7 ppm vodika).

Fig. 3:

Load-deformation diagram obtained at slow-strain-rate tension test of steel with yield strength of 1300 MPa. (a) without hydrogen (less than 0,05 ppm) and (b) 24 hours after hydrogen charging (appr. 0,7 ppm hydrogen).

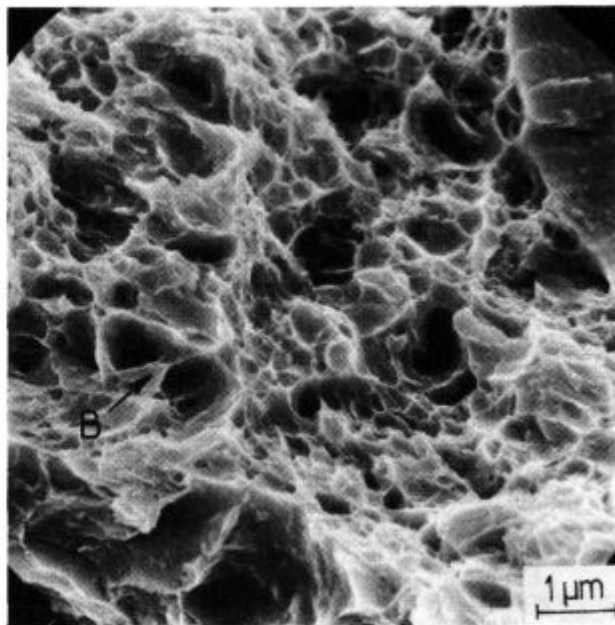
V diagramu sila-deformacija na **sliki 3** je prikazana odvisnost med silo in raztežkom pri počasnem natezanju jekla s trdnostjo ca. 1300 MPa. Odvisnost, označena z a), velja za jeklo brez vodika (pod 0,05 ppm), z napetostjo tečenja 1070 MPa, trdnostjo 1286 MPa, enakomernim raztežkom $e_u = 6\%$ in kontrakcijo $Z = 49\%$, medtem ko velja odvisnost, označena z b), za jeklo istega trdnostnega razreda, ki pa je bilo natežano 24 ur po vodičenju (ca. 0,7 ppm vodika). V tem primeru smo namerili napetost tečenja 1090 MPa, trdnost 1284 MPa, enakomerni raztežek $e_u = 5,6\%$ ter kontrakcijo $Z = 39\%$.

Mikrofraktografske preiskave prelomnih površin navodičenih natežnih preizkušancev kažejo, da z vodikom inducirani lom pri počasnem natezanju takšnih preizkušancev ne ostane povsem duktilnega tipa, celo pri preizkušancih z relativno nizko napetostjo tečenja ne (**slika 4**). Pri višji napetosti tečenja so prelomne površine navodičenega ter počasni natežanega jekla mešane narave; poleg kvazicepilnih ploskev najdemo na prelomnih površinah tudi jamičasta duktilna področja ter številne grebene, nastale s trganjem (**slika 5**).

5. RAZPRAVA

Analiza rezultatov mehanskih preizkusov (**Tabela 1**) kaže, da je lomna žilavost K_{IC} , s katodnim polariziranjem navodičenega jekla z visoko trdnostjo, le malo manjša od lomne žilavosti enakega jekla brez vodika, kot o tem tudi sicer lahko sklepamo iz diagrama na **sliki 1**.

Počasnejše natezanje pri jeklu brez vodika ne povzroči kakšnih opaznejših sprememb, medtem ko se pri

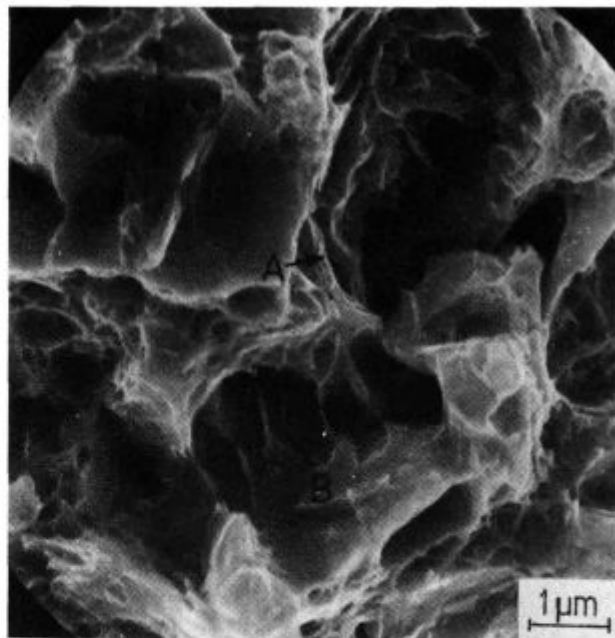


Slika 4:

Jamičasta duktilna prelomna površina s posameznimi kvazicepilnimi detajli (B) pri vodičenem in počasi natežanem jeklu z napetostjo tečenja ca. 900 MPa.

Fig. 4:

Dimpled ductile fracture area with some quasicleavage details (B) in hydrogen-charged and slow-strain-rate tested steel with yield strength of 900 MPa.



Slika 5:

Mešana oblika preloma vodičenega jekla z napetostjo tečenja ca. 1070 MPa.

Poleg cepilnih oziroma kvazicepilnih ploskev (B) je na prelomni površini moč zaslediti tudi jamičasta duktilna področja ter številne grebene, nastale s trganjem.

Fig. 5:

Mixed fracture mode on hydrogen-charged steel with yield strength of 1070 MPa.

Besides cleavage and quasicleavage facets (B), dimpled ductile areas and many tear ridges can also be observed.

navodičenem jeklu močno poslabša lomna duktilnost, t.j. kontrakcija jekla, ne pa tudi enakomerni raztezek, trdnost in napetost tečenja takšnega jekla. Poslabšanje lomne duktilnosti navodičenega jekla pri počasnem natezanju dejansko kaže na obstoj faktorja mejne intenzitete napetosti K_{TH} (K_{HE}). S Hahn-Rosenfieldovo korelacijo (7) izračunane vrednosti K_{TH} dajejo namreč, po substituciji v Gerberichovo enačbo (6), za konstanto β vrednost približno 4100 MPa. Ta vrednost je neodvisna od napetosti tečenja jekla in zato v okviru eksperimentalne natančnosti merjenja res konstantna količina, skladno z Gerberichovim modelom.

Eksperimenti so nadalje pokazali, da je bila uporabljena hitrost natezanja 0,1 mm/min že dovolj majhna, da smo lahko iz poslabšanja lomne duktilnosti navodičenega jekla izračunali take vrednosti faktorja mejne intenzitete napetosti K_{TH} , za katere je β konstanta.

Če upoštevamo, da velikost plastične cone v trenutku loma navodičenega preizkušanca dosega velikost približno polovice vratu preizkušanca ($l=3$ mm), dobimo za $\dot{\epsilon}_c$, upoštevaje hitrost natezanja $v=1,6 \times 10^{-3}$ mm s⁻¹ (0,1 mm/min), vrednost $\dot{\epsilon}_c = v/l = 5,3 \times 10^{-4}$ s⁻¹.

V strokovni literaturi¹⁵ navajajo za nerjavna jekla nekoliko višje vrednosti $\dot{\epsilon}_c$, približno 10^{-1} s⁻¹. Raziskava Nakana in sodelavcev¹⁶, opravljene s počasnim natezanjem vodičenega jekla z napetostjo tečenja 500 MPa, pa kažejo, da se pri zadostni koncentraciji vodika v jeklu kontrakcija jekla asimptotično približa neki znižani vrednosti že pri kritični hitrosti deformacije $\dot{\epsilon}_c = 10^{-4}$ s⁻¹, to pa je že velikostni red naših izmerjenih vrednosti. Ta hitrost deformacije je namreč že dovolj majhna, da Cottrellovi oblaki vodikovih atomov lahko potujejo skupaj z dislokacijami globoko v plastično cono nateznih preizkušancev.

Diagram na sliki 3 potrjuje, da vodik ne vpliva bistveno na mobilnost dislokacij v zgodnjih fazah deformacijskega procesa pri natezanju, saj skoraj ne učinkuje na napetost tečenja, trdnost in enakomerni raztezek jekla, pač pa le na kontrakcijo jekla. Vodik torej spreminja obliko diagrama sila-deformacija še ole pojavljanja plastične nestabilnosti dalje, kar se dobro ujema z navedbami iz različnih literaturnih virov¹⁷⁻²⁵. Po teh navedbah vodik ne vpliva niti na zgodnje nukleiranje mikropor, niti na gostoto mikropor, ko se stopnja deformacije približuje lomni deformaciji. Očitno je zato vpliv vodika zaznaven še v fazi rasti mikropor in/ali fazi njihovega združevanja. Do pospešene rasti in koalescence mikropor v tej fazi pa lahko pride tudi z mehanizmom ločevanja prostih površin, na katerih je adsorbiran vodik²⁶. Na sliki 6 je shematsko prikazana rast in koalescenca mikropor vzdolž meje dveh kristalnih zrn. Mehanizem koalescence mikropor z ločevanjem prostih površin, na katerih je adsorbiran vodik, prične delovati, ko se oblikuje troosno napetostno stanje v zoženem delu nateznega preizkušanca. Posledica tega je že opisano "zgoščevanje" zadnje faze plastične deformacije pri počasnem natezanju navodičenega jekla.

Mikrofraktografske preiskave samo še ilustrirajo pravkar opisani mehanizem loma. Pojasnjujejo namreč lome jamičaste duktilne vrste, pri katerih pa kažejo stene in dna jamic posamične mikromorfološke značilnosti cepilnega oziroma kvazicepilnega loma. Res smo tudi pri naših raziskavah vodičenega in počasi nateznega jekla višjega trdnostnega razreda opazili poleg duktilnih jamičastih področij še trganja (tearing), ki so sicer značilna za jekla z zadostno duktilnostjo in dovolj majhno napetostjo tečenja, da do porušitve lahko pride s plastično deformacijo. Poleg detajlov takšne vrste pa smo opazili na prelomnih površinah tudi področja kvazicepilne narave, čisto na samem obrobju večjih in globljih, lijakasto

4. RESULTS

The mechanical properties of hydrogen-charged as well as hydrogen uncharged steel (less than 0,05 ppm) are presented in Table 1. The fracture toughness of steel K_{IC} , calculated according to the Hahn-Rosenfield correlation (7) on the basis of conventional tension tests made at a crosshead speed of 1 mm/min, as well as the threshold stress intensity factor K_{TH} of cathodic charged steel, also calculated using equation (7), but on the basis of results obtained at a crosshead speed of 0,1 mm/min, are also shown in Table 1.

The values of constant β are also given in Table 1. These were calculated using equation (10), on the basis of slow-strain-rate tensile test data.

The load-deformation diagram (Fig. 3) shows the relation between load and elongation at slow-strain-rate tension of steel with a tensile strength of approx. 1300 MPa. Curve a) denotes the uncharged steel (less than 0,05 ppm hydrogen), having a yield strength of 1070 MPa, tensile strength of 1286 MPa, uniform elongation $e_u=6\%$ and reduction of area $Z=49\%$, whereas Curve b) denotes hydrogen-charged steel (approx. 0,7 ppm hydrogen) of the same strength class, being tested 24 hours after it had been charged. In this case the yield strength of 1090 MPa, tensile strength of 1284 MPa, uniform elongation $e_u=5,6\%$ and reduction of area $Z=39\%$ were measured.

The microfractographic examinations of fracture surfaces of hydrogen-charged specimens confirm that hydrogen-induced fracture at slow-strain-rate tension does not remain predominantly ductile, even in specimens with a relatively low yield strength (Fig. 4). The fracture surfaces of hydrogen-charged steel with higher yield strength, stretched at slow-strain-rate tension, are of mixed mode. In addition to quasicleavage details, ductile dimpled areas and numerous tear ridges have also been observed (Fig. 5).

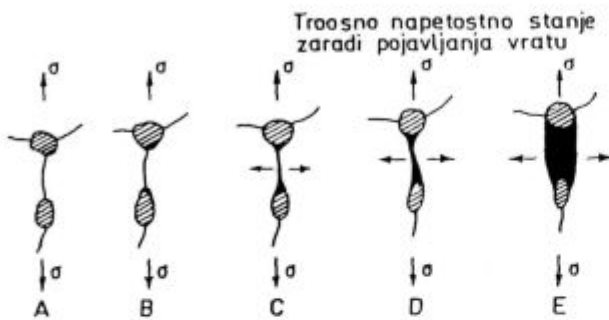
5. DISCUSSION

The analysis of mechanical testing data (Table 1) shows that the fracture toughness K_{IC} of hydrogen-charged high-strength steel is only slightly lower than that of the uncharged steel, which can also be concluded from the diagram in Fig. 1.

The slow-strain-rate tension of uncharged steel does not provoke any noticeable changes, whereas that of hydrogen-charged steel strongly decreases the fracture ductility, i.e. the reduction of area, but does not affect the uniform elongation, tensile strength and yield strength of such steel. The deterioration of fracture ductility of hydrogen-charged steel at slow-strain-rate tension indicates the existence of the threshold stress intensity factor K_{TH} (K_{HE}). Namely, the K_{TH} - values, calculated with the Hahn-Rosenfield correlation (7) after being substituted into Gerberich's equation (6), give an approximate value of 4100 MPa for the β -constant. Within the experimental error of the measurements, the obtained value is constant and, in accordance with Gerberich's model, independent of the yield strength of steel.

The experiments further showed that the applied crosshead speed of 0,1 mm/min was sufficiently low to enable the calculation of K_{TH} - values from the decrease in fracture ductility of hydrogen-charged steel, i.e. the calculation of K_{TH} - values for which β is a constant.

Considering that the size of the plastic zone of a hydrogen-charged specimen is approximately half of the neck diameter ($l=3$ mm) at fracture, the crosshead speed is $v=1,6 \times 10^{-3}$ mm s⁻¹ (0,1 mm/min), then a value of $\dot{\epsilon}_c = v/l = 5,3 \times 10^{-4}$ s⁻¹ is obtained.



Slika 6:

Shematski prikaz nastajanja por, njihove rasti in koalescence vzdolž meja zrn, na katerih je adsorbiran vodik /lit. (26)/.

Fig. 6:

Schematic representation of microvoid formation, growth and coalescence along grain boundaries where hydrogen is adsorbed (Ref. 26).

oblikovanih jamic (slika 4, detajl B), pa tudi kot povsem samostojna plitvejša področja.

6. SKLEPI

Na osnovi opravljenih raziskav smo ugotovili, da izgubo lomne duktilnosti pri počasnem natezanju navdichenega jekla z visoko trdnostjo lahko uspešno izkoristimo za kvantitativno določevanje faktorja mejne intenzitete napetosti K_{TH} (K_{HE}). Ugotovili smo namreč, da majhne koncentracije vodika (pod 1 ppm) v jeklu, ki je bilo navdicheno s katodnim polariziranjem, ne vplivajo bistveno na lomno žilavost, merjeno pri običajnih hitrostih natezanja (1 mm/min). Počasno natezanje (0,1 mm/min) navdichenega jekla z visoko trdnostjo pa poslabša lomno duktilnost, kar nakazuje obstoj faktorja mejne intenzitete napetosti K_{TH} . Z izračunanjem faktorjev K_{TH} s pomočjo Hahn-Rosenfeldove korelacije (7) in vstavljanjem teh vrednosti v Gerberichovo enačbo (6) smo ovrednotili parameter β /enačba (10), tabela 1/. Dobili smo konstantno vrednost okoli 4100 MPa, neodvisno od napetosti tečenja jekla, kot to tudi zahteva Gerberichov model za K_{TH} .

Mikrofraktoografske preiskave prelomnih površin počasi natezanega vodičenega jekla z visoko trdnostjo kažejo, da je prelom lokalno še vedno tudi duktilne vrste. Kljub detajlom kvazicepilne narave smo v vseh primerih našli še duktilne grebene, nastale s trganjem, in jamičasta področja duktilnega tipa. Kvazicepilna oblika loma na obrobju večjih in globljih lijakasto oblikovanih jamic dokazuje, da so le-te rasle in se medsebojno zlivale tudi z mehanizmom ločevanja prostih površin, na katerih je bil adsorbiran vodik.

Professional literature¹⁵ quotes somewhat higher $\dot{\epsilon}_c$ - values for stainless steels, approximately $10^{-1} s^{-1}$. However, the investigations performed by Nakano and co-workers¹⁶ on hydrogen-charged steel with yield strength of 500 MPa using slow-strain-rate measurements show that at sufficient concentration of hydrogen in steel the reduction of area asymptotically approaches the reduced value already at a critical deformation rate of $\dot{\epsilon}_c = 10^{-4} s^{-1}$, whose magnitude is of the same order as found in our investigations. This deformation rate is, in fact, low enough to enable the Cottrell atmosphere of hydrogen atoms pinned on dislocations to penetrate deep into the plastic zone of tensile specimens.

The diagram on Fig. 3 confirms that hydrogen has no essential influence on the mobility of dislocations in earlier phases of the deformation process at tension. It has almost no effect on the yield strength, tensile strength and uniform elongation of steel, but only on the reduction of area. Thus hydrogen changes the shape of a load-deformation diagram only after the appearance of plastic instability, as already found by a number of authors¹⁷⁻²⁵. According to these sources, hydrogen has no effect on the early nucleation of microvoids, nor on microvoid density, when the deformation approaches the fracture deformation. Therefore, the effect of hydrogen becomes obvious only at the stage of microvoid growth and/or during their coalescence. The growth of microvoid and their coalescence can also be accelerated by a mechanism of separation of internal interfaces where hydrogen is adsorbed²⁵. The growth and coalescence of microvoids along the grain boundary are schematically shown in **Figure 6**. The mechanism of microvoid coalescence and the separation of internal interfaces due to adsorbed hydrogen becomes operative when the triaxial stress state in the narrow neck of the tensile specimen is formed, resulting in the previously described "condensation" of the last stage of plastic deformation at slow-strain-rate tension of hydrogen-charged steel.

The microfractographic investigations are an additional illustration of above-mentioned fracture mechanism. They explain the ductile-dimpled types of fracture in which the walls and bottoms of dimples exhibit individual micromorphological characteristics of the cleavage or quasi-cleavage type of fracture. It is true that our investigations of hydrogen-charged high-strength steel at slow-strain-rate also showed, in addition to ductile-dimpled areas, tearing regions typical for steels with sufficiently high ductility and yield strength low enough that the fracture may be the result of plastic deformation. Besides the details of such ductile types, we also observed quasicleavage areas on fracture surfaces, most often on the very periphery of larger, deeper funnel-type dimples (Fig. 4, detail B) and also as entirely independent shallow regions.

6. CONCLUSIONS

On the basis of the performed investigations, we have ascertained that the loss of fracture ductility at slow-strain-rate tension of hydrogen-charged high-strength steel can be successfully used for the quantitative determination of the threshold stress intensity factor K_{TH} (K_{HE}). It was established that small concentrations of hydrogen (less than 1 ppm) in cathodically-charged steel have no substantial influence on the fracture toughness, as measured at conventional strain-rate (1 mm/min). However, the slow-strain-rate (0,1 mm/min) of hydrogen-charged high-strength steel weakens the fracture ductility, which reflects the existence of the threshold stress intensity factor K_{TH} . The parameter β

/Eq. (10), Table 1/ was determined by inserting the K_{TH} - values, calculated using the Hahn-Rosenfield correlation (7), into Gerberich's equation (6). We thus obtained a constant value of about 4100 MPa, independent of the yield strength of steel, as requested by Gerberich's model for K_{TH} .

Microfractographic investigations of fracture surfaces of highstrength hydrogen-charged steel tested at slow-strain-rate indicate that, locally, the fracture is still of ductile type. Despite the quasicleavage details, ductile ridges as a result of tearing as well as ductile dimpled areas were found in all cases. The quasicleavage type of fracture on the periphery of larger, deeper and funnel-type dimples proves that the growth and coalescence of voids are also the consequence of the mechanism causing the separation of internal interfaces where hydrogen is adsorbed.

LITERATURA / REFERENCES

1. C.S. Kortovich in E.A. Steigerwald, Eng. Fract. Mech., 4, 637 (1972).
2. G.L. Hanna, A.R. Troiano in E.A. Steigerwald, Trans. of the ASM, 57, 658-671 (1964).
3. New hydrogen-embrittlement test, Advanced Materials and Processes Inc., Metal Progress, 7, 10-11 (1988).
4. K. Farrell in A.G. Quarrell, J. Iron Steel Inst., 202, 1002 (1964).
5. H. Morimoto in Y. Ashida, Trans. ISIJ, 23, B-352 (1983).
6. H. Wagenblast in H.A. Wriedt, Metall. Trans., 2, 1393-1397 (1971).
7. J.O'M. Bockris, W. Beck, M.A. Genshaw, P.K. Subramanyan in F.S. Williams, Acta metall., 19, 1209-1218 (1971).
8. H. Peisl in Hydrogen in Metals, Topics in Applied Physics, Ed.: G. Alefeld and J. Volkl, vol. 28, 53-74 (1978).
9. L.C.M. Li, R.A. Oriani in L.S. Darken, Z. Phys. Chem., 49, 271 (1966).
10. W.W. Gerberich in Effect of Hydrogen in high-strength and martensitic steels, Hydrogen in Metals, ASM-Ohio, 115 (1974), kot tudi:
W.W. Gerberich in S.T. Chen, Metall. Trans., 6A, 271 (1975).
11. C.D. Kim in A.W. Lognow, Corrosion, 24, 313 (1968).
12. G.T. Hahn in A.R. Rosenfield, Sources of Fracture Toughness: The Relation between KIC and the Ordinary Tensile Properties of Metals, Applications Related Phenomena in Titanium Alloys, ASTM STP 432, 5-32, Philadelphia, (1968).
13. G.T. Hahn in A.R. Rosenfield, Metall. Trans., 6A, 653-668 (1975).
14. G.T. Hahn in A.R. Rosenfield, Trans., ASM, 59, 909 (1966).
15. M.B. Whiteman in A.R. Troiano, Corrosion, 21, 53-56 (1965).
16. K. Nakano, M. Kanao in T. Aoki, Trans. of National Research, Institute for Metals, 29, No. 2, 34-43 (1987).
17. R. Garber, M. Bernstein in A.W. Thompson, Scr. Metall., 10, 341-345 (1976).
18. A.S. Argon in J. Im, Metall. Trans., 6A, 839-851 (1975).
19. J.R. Rice in D.M. Tracey, J. Mech. Phys. Solids, 17, 201-217 (1969).
20. D.M. Tracey, Eng. Fract. Mech., 3, 301-315 (1971).
21. A.S. Argon, J. Im in R. Safoglu, Metall. Trans., 6A, 825-838 (1975).
22. C.D. Beachem, Metall. Trans., 3, 437-451 (1972).
23. T.D. Lee, T. Goldenberg in J.P. Hirth, Metall. Trans., 10A, 199-208 (1979).
24. In-Gyn Park in A.W. Thompson, Metall. Trans., 21A, 465-477 (1990).
25. D. Kwon in R.J. Asaro, Metall. Trans., 21A, 117-134 (1990).
26. H. Cialone in R.J. Asaro, Metall. Trans., 10A, 367-375 (1979).